ISSN 1075-7015, Geology of Ore Deposits, 2016, Vol. 58, No. 8, pp. 697–710. © Pleiades Publishing, Ltd., 2016.
Original Russian Text © M.N. Ankushev, V.V. Zaykov, V.A. Kotlyarov, M.E. Romanenko, 2015, published in Zapiski Rossiiskogo Mineralogicheskogo Obshchestva, 2015, No. 5, pp. 76–96.

MINERALS AND MINERAL ASSEMBLAGES

Chrome Spinels and Accessory Mineralization in the Weathering Crust of the Vladimir Deposit, Varshavsky Ultramafic Massif, Southern Urals

M. N. Ankushev[a], *, V. V. Zaykov[a], V. A. Kotlyarov[a], and M. E. Romanenko[b]

[a] *Institute of Mineralogy, Ural Branch, Russian Academy of Sciences, Ilmensky Reserve 1, Miass, 456317 Russia*
[b] *Novosibirsk State University, Novosibirsk-90, ul. Pirogova 2, 630090 Russia*
**e-mail: ankushev_maksim@mail.ru*

Received December 12, 2014

Abstract—The paper presents the characteristics of chrome spinels from an ore-bearing packet of the Vladimir chromite deposit. Three main types of chrome spinels are distinguished by morphology and chemical composition: medium-chrome ore-forming, high-chrome transformed, and low-chrome relict accessory. The significant role of weathering conditions is expressed in alteration of accessory chrome spinel. The formation of high-chrome spinels is explained by the hydrothermal effect of the Varshavsky granitoid massif with accompanying dikes and talc–carbonate metasomatic rocks. Characteristic accessory minerals are represented by native gold and nickel, millerite, pentlandite, chalcopyrite, maucherite, PGE sulfides, and picroilmenite.

Keywords: accessory chrome spinels, metamorphism of chrome spinels, PGE sulfides, picroilmenite
DOI: 10.1134/S1075701516080031

INTRODUCTION

The Varshavsky ultramafic massif and related chromite deposits are localized in the southern Chelyabinsk region 30–37 km south of Kartaly town. The Vladimir chromite deposit is the most attractive object with respect to research of Cr-spinel. The open pit at this deposit is not underwater and affords the opportunity to thoroughly study orebody fragments and related mineralization hosted in the weathering crust. The objective of our work is to provide insight into the distribution of Cr-spinels and accessory minerals in the ore-bearing packet affected by intense weathering, as well as the composition of ore-forming and accessory Cr-spinels, accompanying sulfide and noble-metal mineralization, and the role of supergenesis in the mineralogy of the ore-bearing packet.

METHODS

The factual data were obtained during fieldworks in 2009–2013, when we geologically mapped the open pit at the deposit and documented the ore-bearing serpentinite packet in detail. We collected samples of various ultramafic rocks, including varieties with Cr-spinel crystals, banded chromite ore, and ore veins. Polished sections with Cr-spinel crystals and thin sections of host rocks were optically examined with an Axiolab Carl Zeiss and Olympus BX-51 microscopes. The chemical composition of Cr-spinel was determined on REMMA-202M SEM equipped with X-ray LZ-5 EDS (SiLi detector, resolution 140 eV); accelerating voltage 20 or 30 kV; probe current 4–6 nA. We used standards for pure metals (MICRO-ANALYSIS CONSULTANTS LT, LTD, X-RAY MICROPROBE STANDARDS, REGISTERED STANDARD NUMBER 1362) or standard synthetic or natural minerals (ASTIMEX SCIETIFIC LIMITED, MINM25-53. Mineral Mount Serial No: 01-044), analyst V.A. Kotlyarov. The chemical composition of certain Cr-spinels was established with JEOL-733 SEM (Institute of Mineralogy, Ural Branch, Russian Academy of Sciences), the standard is chromite 79/62, accelerating voltage is 20 kV, and the probe current is 30 nA; analyst E.I. Churin. The compositions of PGE sulfides were measured with JEOL JSM-7001F SEM at South Urals State University (analysts O.V. Samoilova and M.V. Sudarikov); add-in software standards were used. The common parameters of Cr-spinel: #Cr = Cr/(Cr + Al) and #Mg = Mg/(Mg + Fe^{2+}) were calculated based on atomic quantities. Formulae of minerals were calculated by the anionic method: the formula of Cr-spinel is based on four O atoms; millerite, on one S atom; pentlandite, on eight S atoms; chalcopyrite, on two S atoms; maucherite, on eight As atoms; and picroilmenite, on four O atoms.

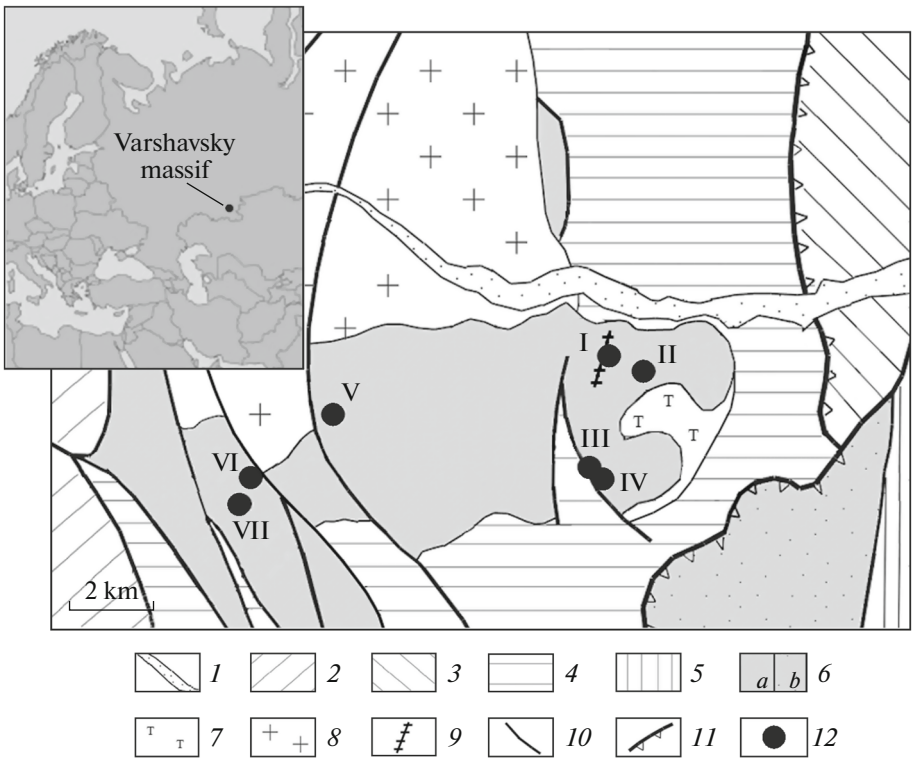

Fig. 1. Index map and schematic geological map of South Varshavsky ultramafic massif and adjacent territory, after Moseichuk (2009, unpublished report). (*1*) Recent alluvial sediments; (*2*) metasedimentary rocks of Lower Ordovician Rymnik Formation; (*3*) volcanic and sedimentary rocks of Lower–Middle Ordovician Sargazy Sequence; (*4*) metaterrigenous rocks of Lower Carboniferous Bredy Formation; (*5*) sedimentary rocks of Lower Carboniferous Birgilda Formation; (*6*) ultramafic massifs: (*a*) South Varshavsky and (*b*) Gogino; (*7*) metasomatic talc–carbonate rock; (*8*) Varshavsky granitic pluton; (*9*) granite porphyry dike; (*10*) steeply dipping fault; (*11*) thrust fault; (*12*) chromite deposits and occurrences (numerals in figure): I, Vladimir; II, Varshavsky-2; III, East Varshavsky; IV, Pavel; V, Bakhchevaya Gora; VI, Evdokiya; VII, Raisa.

GEOLOGICAL POSITION AND STRUCTURE OF THE VLADIMIR DEPOSIT

The deposit is located at the eastern flank of the Middle Paleozoic Varshavsky ultramafic massif, which extends 15 km in a nearly latitudinal direction (Fig. 1). Seven small deposits are known therein, and the Varshavsky East deposit is the largest (38 kt chromite ore with 46–58 wt % Cr_2O_3 in massive ore and 36–45 wt % in impregnated ore (Ovchinnikov, 1998). An important feature of the ore field is the Late Paleozoic granitic pluton accompanied by numerous dikes and aposerpentinite talc–carbonate metasomatic rocks.

The chromite mineralization of the Varshavsky massif was established in 1911 with the discovery of the Raisa and Evdokia deposits in its western part. Since then, prospecting, exploration, and mining for chromites resumed up to the middle 1940s, periodically intensifying and, conversely, being completely interrupted. These works were especially intense in 1928–1931, when they were related to production activity of the specially created Bashgorpromkontora Enterprise. The Vladimir deposit was discovered in 1929 and mined with a small open pit in 1929–1931 by the Bashchromite Enterprise and then by the Chelyabinsk Electrometallurgical Combine in 1996–2000 (Ivanushkin, 2006).

The ore bodies are hosted in intensely weathered brown apoharzburgite serpentinite dissected with the network of magnesite veinlets. The weathering crust began to form in the Triassic and has continued up to now (Sigov, 1969). The residual weathering crust is mainly a linear type. The areal weathering crust of the full profile has been scoured, and only its deep roots are still retained as zones of disintegration and local leaching. The weathering crust comprises (from top to bottom) chestnut-colored clay enriched in hydrogoethite and secondary cherty rocks; nontronite clay with hydrogoethite; and a disintegration zone composed of serpentinite rubble and weathered serpentinite (Ivanushkin, 2006).

The open pit is 45 m long, 20–25 m wide, and 9 m at maximum depth (Fig. 2). Chromite orebody fragments are localized at the north-eastern open pit wall, where a column of ore-bearing packet has formed (Fig. 3). The packet occurs as a periclinal closure of an anticline.

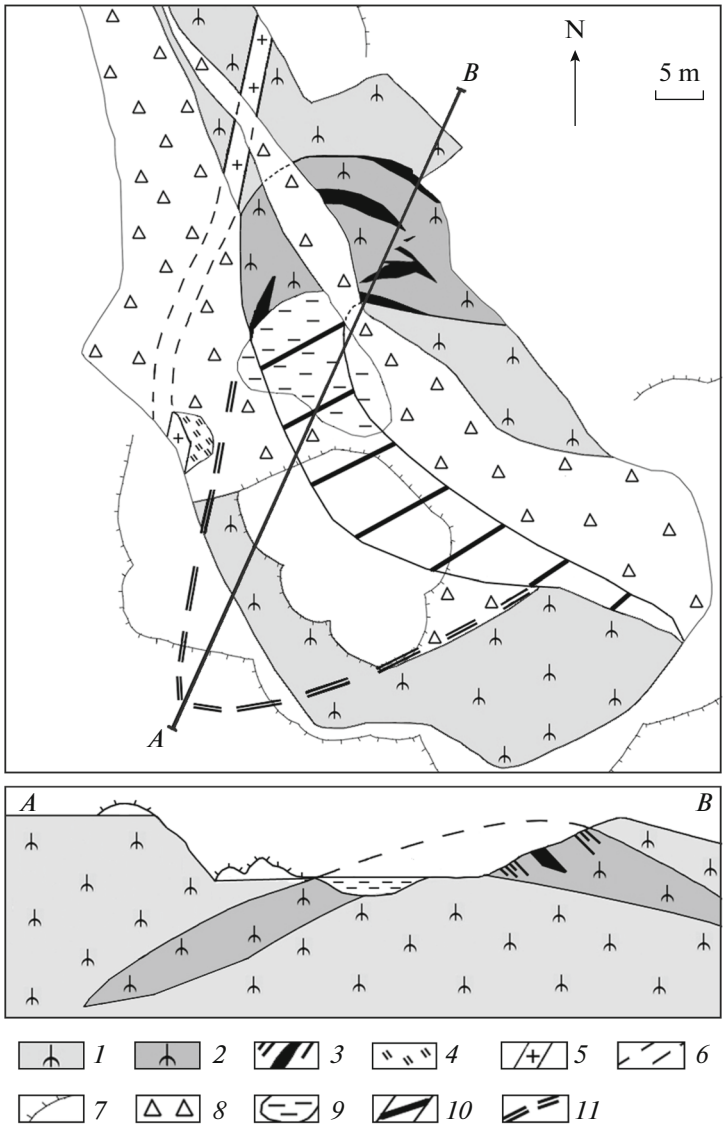

Fig. 2. Schematic geological map of open pit and section *A*–*B* across Vladimir deposit. Data of Ivanushkin (2006) are used. (*1*) weathered serpentinite with network of magnesite veinlets; (*2*) ore-bearing packet of serpentinites various in degree of weathering; (*3*) fragments of chromite orebodies; (*4*) chloritolite; (*5*) granite porphyry dike; (*6*) inferred boundaries of granite porphyry dike; (*7*) dump boundary; (*8*) talus; (*9*) open-pit lake; (*10*) boundary of mined-out ore lode; (*11*) projection of south-western flank of ore lode on horizontal plane (residuary reserves of ore bodies).

In the column of the ore-bearing packet, nine units are represented by antigorite, chrysotile, and antigorite–bastite–chrysotile serpentinites with ore lenses and Cr-spinel impregnations. Samples for study of Cr-spinels and accessory minerals have been taken from each unit. Units I, III, V, VII, and IX are penetrated by networks of magnesite veinlets 1–10 cm in thickness.

Unit I is composed of weathered antigorite–chrysotile serpentinite brown in color. Grains of accessory Cr-spinel are 0.1–0.5 mm in size; their total content in rock is 0.5–2.0%. Cr-spinel is altered beginning with Cr-magnetite rims and frequently up to complete replacement of a grain with Cr-magnetite.

Unit II includes fragments of banded orebodies 0.4–0.6 m in thickness and a few meters long. The ore varies from low-grade with up to 30% Cr-spinel in rock to a densely impregnated variety (70%) and massive ore containing 90% Cr-spinel. Chromite grains are subhedral without magnetite rims; Cr-magnetite sporadically develops in intragranular fractures. The grain size is 0.8–1.0 mm. The banded ore is incorporated into the antigorite–chlorite matrix.

Unit III is identical to Unit I. The weathered antigorite–chrysotile serpentinite is a host rock. Grains of accessory Cr-spinel are 0.3–0.7 mm in size, and their content in rock is 1–3%.

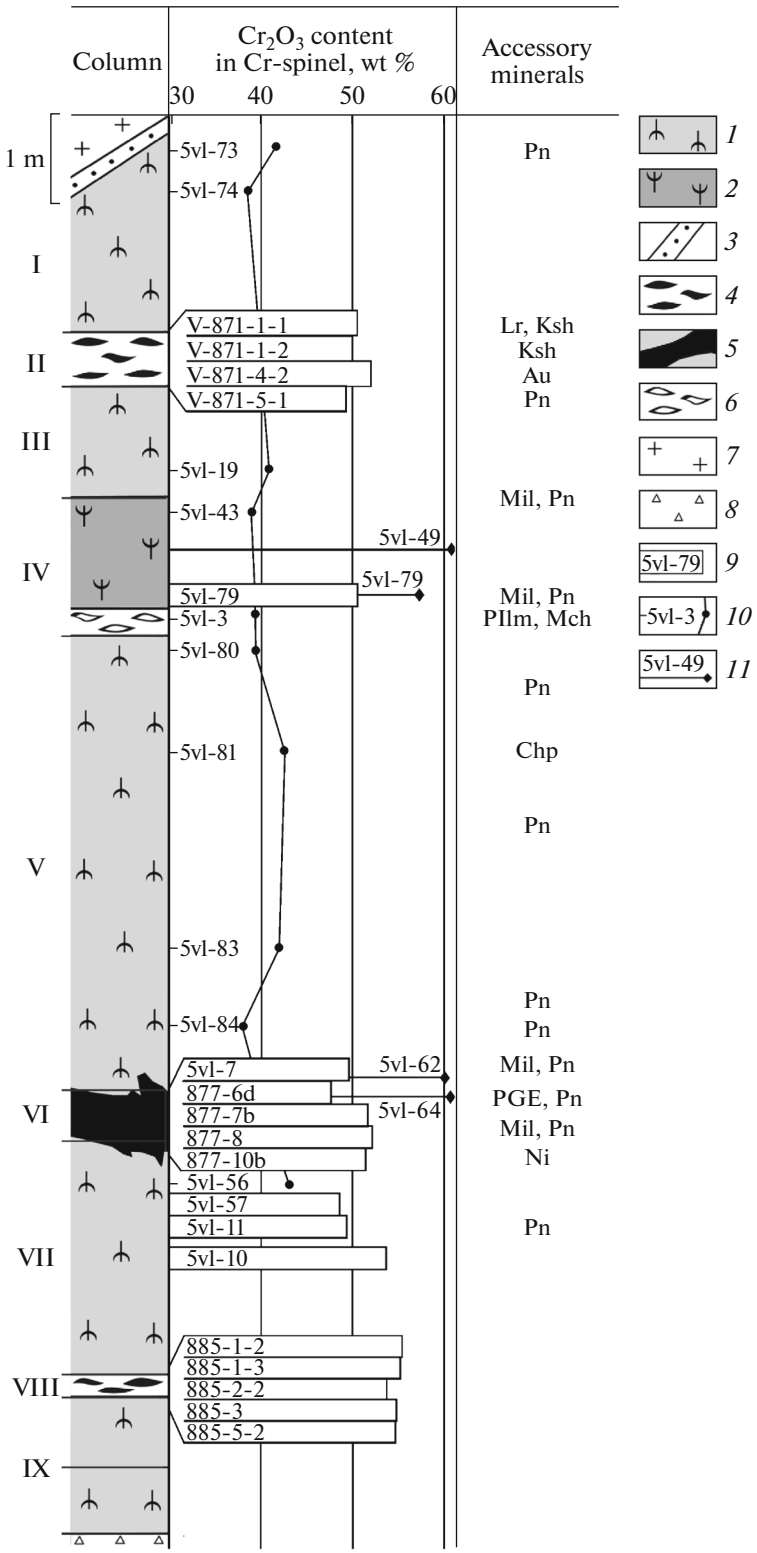

Fig. 3. Ore-bearing packet column of Vladimir deposit. (*1*) weathered antigorite–chrysotile serpentinite with network of magnesite veinlets; (*2*) antigorite serpentinite; (*3*) exocontact zone of dike; (*4*) banded ore; (*5*) ore vein; (*6*) chlorite–chromite veinlets; (*7*) granite porphyry dike; (*8*) talus; (*9–11*) Cr_2O_3 content in: (9) ore Cr-spinel, (*10*) accessory Cr-spinel, (*11*) latticed Cr-spinel. Accessory minerals (literal symbols in figure): Pn, pentlandite; Lr, laurite; Ksh, kashinite; Au, native gold; Mil, millerite; Pilm, picroilmenite; Mch, maucherite; Chp, chalcopyrite; PGE, platinum group elements; Ni, native nickel.

Unit IV is represented by a body of green antigorite serpentinite with chrysotile, chlorite, and chromitite veinlets. The body, 1–2 m thick and 20 m long, is distinct against the weathered chrysotile serpentinites of adjacent units. Antigorite is tabular and pectinate. Chrysotile and chromite–chlorite veinlets are localized in fracture zones and marginal parts of the body. Serpentinite contains accessory Cr-spinel (1–7%) and thin chromite–chlorite bands containing up to 80% Cr-spinel. Chlorite is distinguished by an admixture of 1.6–6.2% Cr_2O_3 (Cr-clinochlore).

Unit V is identical to units I and III and characterized by the most abundant magnesite veinlets. Cr-spinel is accessory (content 0.2–3%, grain size 0.2–0.5 mm).

Unit VI is represented by an ore vein 1–2 m thick and more than 6 m in extent. The orebody, which is bounded by sharp contacts and complicated by short offsets, is composed of massive and densely impregnated ore. The Cr-spinel content in impregnated ore is 50–60% and reaches 80% in massive ore. The intergranular space is filled with serpentinite, chlorite, and carbonates. Cr-spinel in ore vein does not differ in morphology and grain dimensions from the banded ore. The grains are subhedral and unaltered, without magnetite rims. The grain size is 0.5–1.0 mm.

Unit VII consists of weathered antigorite–chrysotile serpentinite brown in color. Cr-spinels in this unit are both accessory (with magnetite rims) and occur as small ore veinlets up to a centimeter in thickness, which are composed of unaltered Cr-spinel. The grain size of accessory Cr-spinel is 0.5–0.8 mm and their content in ore is 1–3% (up to 10% in zones with ore veinlets).

Unit VIII is composed of chrysotile–bastite–antigorite serpentinite with loop structure and contains fragments of banded orebodies 0.5–0.7 m in thickness and a few meters in extent. Boundaries of orebodies are diffuse, and amount of Cr-spinel grains widely varies. The Cr-spinel content reaches 70%. Cr-spinels are unaltered or slightly altered. Magnetite rims at margins of Cr-spinel grains are observed in low-grade impregnated ore. Grain size is 0.8–1.0 mm.

Unit IX is composed of weathered antigorite–chrysotile serpentinite brown in color. Accessory Cr-spinel grains are 0.2–0.5 mm in size and 1–5% in their content; they are completely replaced with Cr-magnetite and magnetite proper.

A granite porphyry dike is exposed in the northern part of the ore-bearing packet. Phenocrysts are represented by plagioclase, quartz, K-feldspar, and hornblende replaced with chlorite and biotite. The groundmass is allotriomorphic-granular; the structure is glomeroporphyritic. The dike locally underwent metasomatic alteration (saussuritization of plagioclase, occurrence of actinolite). The rocks are intensely silicified. The dike is contoured by altered contact zones (20–30 cm) represented by light green antigorite and dark brown dense serpentinite (up to 0.5 m) devoid of carbonate veinlets. Antigorite in light green serpentinite is tabular; dark brown serpentinite is characterized by a loop structure and consists of pectinate antigorite and ophite. Tremolite occurring in the contact zone is represented by radiaxial aggregates up to 3–5 cm in size.

CHEMICAL COMPOSITION OF ORE-FORMING AND ACCESSORY Cr-SPINELS

The chemical composition of Cr-spinel from veined and banded ores, as well as accessory Cr-spinel in host ultramafic rocks, has been studied. As a result, three main types of Cr-spinels are distinguished:

(1) medium-chrome ore-forming (CrSp1),

(2) high-chrome latticed (CrSp2), and

(3) low-chrome relict accessory (CrSp3).

The ore-forming Cr-spinel is represented by subhedral slightly fractured grains (Fig. 4). Their chemical composition is as follows (wt %): 49–57 Cr_2O_3, 13–18 Al_2O_3, 8–11 MgO, 20–26 FeO, 0.3–0.7 TiO_2, 0.2–0.4 MnO (Table 1). The lower unit VIII of banded ore differs from the upper unit II in elevated contents of Cr_2O_3 and TiO_2 along with a lower FeO content. Cr-spinel in ore vein has the following chemical composition (wt %): 48–52 Cr_2O_3, 14–18 Al_2O_3, 11–14 MgO, 18–23 FeO, 0.3–0.4 TiO_2, 0.2–0.3 MnO. The densely impregnated Cr-spinel making up thin ore veinlets in units IV and VII are also referred to this type. The ore-forming Cr-spinels (CrSp1) plotted in the classification diagram correspond to alumochromite (Fig. 5).

The second type of Cr-spinel (CrSp2) is much less abundant. These are sporadic latticed xenomorphic or subhedral grains occasionally with corroded boundaries. The grains contain chlorite ingrowths and are characterized by a subgraphic texture. Inclusions of accessory sulfides, arsenides, and oxides occur as well. This Cr-spinel has the following chemical composition (wt %): 57–67 Cr_2O_3, 2–9 Al_2O_3 (rarely up to 12), 4–9 MgO (rarely up to 11), 19–31 FeO, up to 1.0 TiO_2, up to 0.9 MnO, which corresponds to chromite (Fig. 5). This generation of Cr-spinel occurs in marginal parts of ore veins and at contacts of chromite veinlets and stringers of nephrite-like serpentinite. Veinlets completely filled with high-chrome grains have also been recorded at the deposit. Such veinlets are characterized by latticed or spongy texture (unit IV).

Accessory Cr-spinel (CrSp3) is contained in serpentinite in amounts of 0.2–5%. Grains with Cr-magnetite or magnetite rims and rounded relics of Cr-spinel are typical. Cr-spinel has the following chemical composition (wt %): 38–43 Cr_2O_3, 20–25 Al_2O_3, 8–10 MgO, 25–30 FeO, 0.2–0.7 TiO_2, 0.4–0.7 MnO. These concentrations were established from grains with thin rims and correspond to grains where primary Cr-spinel is retained only as relics 10–20 μm in size.

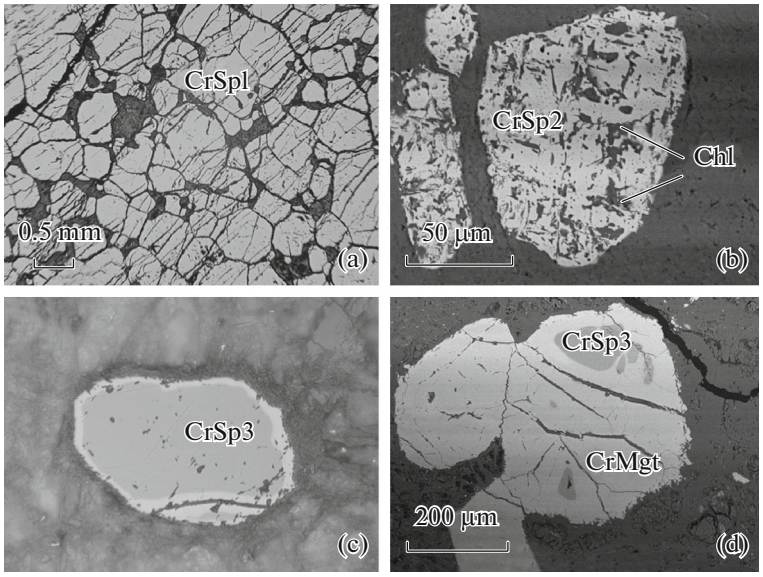

Fig. 4. Cr-spinel from Vladimir deposit: (a) chromitite from banded orebody (sample V-871-1); (b) latticed high-chrome Cr-spinel with chlorite ingrowths (sample 5vl-49); (c) magnetite rim around accessory Cr-spinel (sample 884-7); (d) relict chromite in core of accessory Cr-spinel grain (sample 5vl-43).

In all cases, the boundaries of relics are distinct. The chemical compositions of Cr-spinel (CrSp2) plotted in the classification diagram are localized at boundaries between fields of alumochromite, Cr-picotite, and subferrialumochromite (Fig. 5). A zinc admixture (0.1–0.5%) is occasionally detected in relics of accessory Cr-spinel.

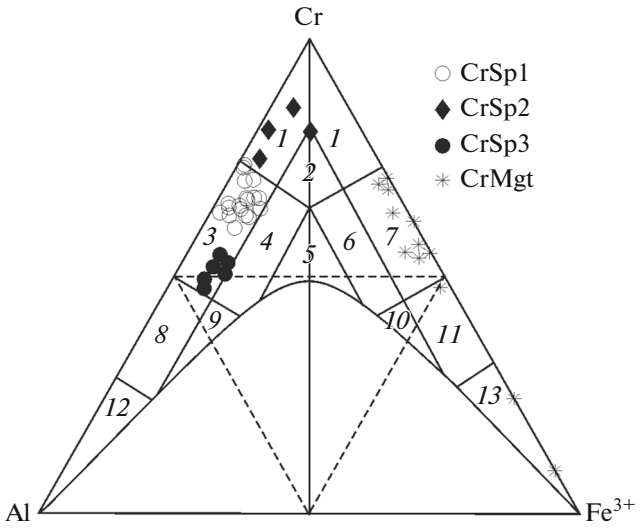

Fig. 5. Chemical compositions of Cr-spinels from Vladimir deposit plotted in classification chart (Pavlov, 1949). (CrSp1) ore Cr-spinel; (CrSp2) latticed Cr-spinel; (CrSp3) relict accessory Cr-spinel. Fields of Cr-spinel compositions (numerals in figure): *1*, chromite; *2*, subferrichromite; *3*, alumochromite; *4*, subferrialumochromite; *5*, ferrialumochromite; *6*, subalumoferrichromite; *7*, ferrichromite; *8,* chrome picotite; *9*, subferrichrome picotite; *10*, subalumochrome magnetite; *11*, chrome magnetite; *12*, picotite; *13*, magnetite.

Cr-magnetite (CrMgt) replaces Cr-spinel grains as rims varying in width and along microfractures. This mineral is very rare in massive, banded, and densely impregnated ores and more abundant in low-grade ore and accessory Cr-spinel up to complete replacement of the grain. Cr-magnetite rims are depleted in Cr, Al, Mg and enriched in Fe, Ti, Mn as compared with ore-forming alumochromite. The Cr_2O_3, Al_2O_3, and MgO contents in the outer part of the rim amount only to a few percent or have been completely removed from Cr-spinel, so that the mineral corresponds to magnetite in composition.

The #Cr = Cr/(Cr + Al) and #Mg = (Mg + Fe^{2+}) values of all analyzed Cr-spinels have been plotted in Irvine's (1965) diagram (Fig. 6). As follows from this plot, the highest #Cr values (0.77–0.90) are inherent to latticed Cr-spinel. They are followed by ore-forming Cr-spinel (0.64–0.74) and the lowest values (0.51–0.58) inherent to the relict accessory type. Cr-spinels hardly vary at all in #Mg. Most values fall in the interval of #Mg = 0.37–0.55. The highest values (0.61–0.66) are related to Cr-spinel from the ore vein.

Cr-spinels from the Vladimir deposit fall into the #Cr versus #Mg field, which characterizes Cr-spinel from peridotite of deepwater trenches except for sporadic samples with the highest #Cr and #Mg. The same tendency is inherent to chromite occurrences in the West Magnitogorsk Zone (Zaykov et al., 2009).

Composition of chrome spinels

No.	Unit	Sample	CrSp type	Number of analyses	Cr_2O_3	Al_2O_3	MgO	ΣFeO	TiO_2	MnO
1	I	5vl-73	CrSp3	10	41.74	22.32	9.67	24.50	0.62	0.38
2		5vl-74		6	38.57	24.56	10.06	24.79	0.50	0.42
3	II	V-871-1-1	CrSp1	9	50.49	14.79	9.03	25.12	0.36	0.40
4		V-871-1-2		8	50.17	14.21	9.28	26.04	0.30	0.42
5		V-871-4-2		9	52.18	14.83	9.83	24.06	0.38	0.38
6		V-871-5-1		9	49.47	15.23	9.95	24.22	0.39	0.25
7	III	5vl-19	CrSp3	34	40.95	20.43	8.24	28.24	0.43	0.47
8	IV	5vl-43	CrSp3	5	39.14	24.19	8.98	26.06	0.46	0.25
9		5vl-49	CrSp2	22	62.23	4.62	6.80	25.16	0.57	0.22
10		5vl3	CrSp3	24	39.52	20.83	7.62	29.72	0.48	0.69
11		5vl-79	CrSp1	3	50.61	17.59	10.89	19.70	0.56	0.55
12			CrSp2	2	57.54	4.42	4.87	30.57	0.49	0.82
13	V	5vl-80	CrSp3	2	39.38	24.56	9.34	24.49	0.58	0.60
14		5vl-81		3	42.25	23.63	9.22	23.51	0.24	0.31
15		5vl-83		8	41.70	23.99	9.88	22.73	0.65	0.31
16		5vl-84		2	37.88	23.22	10.37	26.73	0.44	0.49
17	VI	5vl-7	CrSp1	1	49.75	16.93	8.26	23.74	0.53	0.38
18		5vl-62	CrSp2	1	60.74	8.76	8.81	20.60	–	0.55
19		5vl-64		1	61.78	6.36	6.56	23.76	0.56	0.20
20		877-6d	CrSp1	12	47.70	17.78	10.54	22.90	0.35	0.31
21		877-7b		12	51.73	13.95	13.67	18.32	0.29	0.15
22		877-8		12	52.18	14.31	12.72	19.40	0.31	0.18
23		877-10b		12	51.41	15.91	13.49	18.58	0.39	0.16
24	VII	5vl-56	CrSp3	12	43.13	20.94	9.21	25.27	0.35	0.50
25		5vl-57	CrSp1	12	48.64	17.18	7.95	24.75	0.36	0.37
26		5vl-11		21	49.29	16.96	8.97	23.61	0.54	0.37
27		5vl-10		24	53.63	13.45	7.80	23.94	0.45	0.37
28	VIII	885-1-2	CrSp1	5	56.50	13.35	9.18	20.03	0.59	0.15
29		885-1-3		5	56.26	12.97	8.36	21.01	0.69	0.30
30		885-2-2		5	54.02	12.96	9.23	22.76	0.41	0.36
31		885-3		5	50.65	16.83	9.42	21.73	0.69	0.26
32		885-5-2		5	50.35	18.17	10.59	19.94	0.47	0.20

Analyses (20–23) were carried out on electron microprobe at the Institute of Mineralogy of the Ural Branch of the Russian Academy of Sciences . Dash denotes not detected.

CONCOMITANT ACCESSORY MINERALIZATION

Accessory minerals are represented by native gold and nickel, millerite, pentlandite, chalcopyrite, maucherite, PGE sulfides, and picroilmenite (Fig. 7).

The inclusion of **native gold** has been identified in a fracture at the contact of massive chromite ore and serpentinite in the central part of the ore-bearing packet (unit II, sample 871-4). An elongated gold grain (4 × 12 μm) consists of (wt %): 87–90 Au, 8–11 Ag, 1.7–2.1 Cu.

Native nickel occurs as an elongated grain (3 × 8 μm) at the contact of antigorite serpentinite and the chromite vein (unit IV, sample 5vl-12). The chemical composition of this mineral is (wt %): 93–96 Ni, 4.0–6.5 Cd, and 0.35–0.70 Zn.

Millerite forms somewhat larger aggregates (up to 80 μm) of tabular and lance-shaped grains occasionally intergrown with pentlandite. Millerite inclusions are mainly hosted in ore-forming Cr-spinel. Their chemical composition is (wt %): 58–64 Ni, 33–36 S, up to 7.2 Fe, and up to 0.6 Co (Table 2).

Pentlandite grains are isometric or tabular 5–10 μm in size. This mineral was identified throughout the ore-

Table 1. Chemical composition of Cr-spinel from ore-bearing packet of Vladimir deposit

ZnO	V_2O_3	Total	Crystal chemical formula	#Cr	#Mg
0.47	–	99.70	$\left(Fe^{2+}_{0.55}Mg_{0.46}Mn_{0.01}Zn_{0.01}\right)_{1.03}\left(Cr_{1.05}Al_{0.84}Fe^{3+}_{0.09}Ti_{0.01}\right)_2O_4$	0.56	0.48
–	–	98.89	$\left(Fe^{2+}_{0.55}Mg_{0.48}Mn_{0.01}\right)_{1.03}\left(Cr_{0.97}Al_{0.92}Fe^{3+}_{0.09}Ti_{0.01}\right)_2O_4$	0.51	0.48
–	–	100.19	$\left(Fe^{2+}_{0.58}Mg_{0.44}Mn_{0.01}\right)_{1.03}\left(Cr_{1.32}Al_{0.57}Fe^{3+}_{0.1}Ti_{0.01}\right)_2O_4$	0.70	0.45
–	–	100.41	$\left(Fe^{2+}_{0.58}Mg_{0.46}Mn_{0.01}\right)_{1.05}\left(Cr_{1.31}Al_{0.55}Fe^{3+}_{0.13}Ti_{0.01}\right)_2O_4$	0.70	0.46
–	–	101.66	$\left(Fe^{2+}_{0.55}Mg_{0.47}Mn_{0.01}\right)_{1.03}\left(Cr_{1.33}Al_{0.57}Fe^{3+}_{0.09}Ti_{0.01}\right)_2O_4$	0.70	0.48
–	–	99.50	$\left(Fe^{2+}_{0.54}Mg_{0.49}Mn_{0.01}\right)_{1.04}\left(Cr_{1.29}Al_{0.59}Fe^{3+}_{0.11}Ti_{0.01}\right)_2O_4$	0.69	0.49
0.10	–	98.87	$\left(Fe^{2+}_{0.63}Mg_{0.4}Mn_{0.01}\right)_{1.05}\left(Cr_{1.06}Al_{0.79}Fe^{3+}_{0.13}Ti_{0.01}\right)_2O_4$	0.57	0.41
0.48	–	99.56	$\left(Fe^{2+}_{0.59}Mg_{0.43}Mn_{0.01}\right)_{1.03}\left(Cr_{0.99}Al_{0.91}Fe^{3+}_{0.1}Ti_{0.01}\right)_2O_4$	0.52	0.43
–	–	99.61	$\left(Fe^{2+}_{0.66}Mg_{0.35}Mn_{0.01}\right)_{1.02}\left(Cr_{1.72}Al_{0.19}Fe^{3+}_{0.07}Ti_{0.02}\right)_2O_4$	0.90	0.36
0.18	–	99.03	$\left(Fe^{2+}_{0.65}Mg_{0.37}Mn_{0.02}\right)_{1.05}\left(Cr_{1.03}Al_{0.81}Fe^{3+}_{0.15}Ti_{0.01}\right)_2O_4$	0.56	0.38
–	–	99.91	$\left(Fe^{2+}_{0.48}Mg_{0.52}Mn_{0.01}\right)_{1.01}\left(Cr_{1.28}Al_{0.66}Fe^{3+}_{0.04}Ti_{0.01}\right)_2O_4$	0.66	0.53
–	–	98.69	$\left(Fe^{2+}_{0.76}Mg_{0.26}Mn_{0.03}\right)_{1.05}\left(Cr_{1.65}Al_{0.19}Fe^{3+}_{0.15}Ti_{0.01}\right)_2O_4$	0.90	0.27
0.75	0.30	99.98	$\left(Fe^{2+}_{0.55}Mg_{0.44}Mn_{0.02}\right)_{1.03}\left(Cr_{0.98}Al_{0.91}Fe^{3+}_{0.08}Ti_{0.01}V_{0.01}\right)_2O_4$	0.52	0.45
0.78	0.17	100.11	$\left(Fe^{2+}_{0.56}Mg_{0.43}Mn_{0.01}Zn_{0.02}\right)_{1.02}\left(Cr_{1.05}Al_{0.88}Fe^{3+}_{0.06}Ti_{0.01}\right)_2O_4$	0.55	0.44
0.24	0.32	99.82	$\left(Fe^{2+}_{0.54}Mg_{0.46}Mn_{0.01}Zn_{0.01}\right)_{1.01}\left(Cr_{1.03}Al_{0.89}Fe^{3+}_{0.05}Ti_{0.02}V_{0.01}\right)_2O_4$	0.54	0.47
0.35	0.21	99.67	$\left(Fe^{2+}_{0.54}Mg_{0.49}Mn_{0.01}Zn_{0.01}\right)_{1.06}\left(Cr_{0.96}Al_{0.87}Fe^{3+}_{0.16}Ti_{0.01}V_{0.01}\right)_2O_4$	0.52	0.50
–	–	99.60	$\left(Fe^{2+}_{0.6}Mg_{0.4}Mn_{0.01}\right)_{1.01}\left(Cr_{1.29}Al_{0.65}Fe^{3+}_{0.05}Ti_{0.01}\right)_2O_4$	0.66	0.41
–	–	99.46	$\left(Fe^{2+}_{0.55}Mg_{0.44}Mn_{0.02}\right)_{1.01}\left(Cr_{1.62}Al_{0.35}Fe^{3+}_{0.05}\right)_2O_4$	0.82	0.45
–	–	99.57	$\left(Fe^{2+}_{0.66}Mg_{0.34}Mn_{0.01}\right)\left(Cr_{1.7}Al_{0.26}Fe^{3+}_{0.03}Ti_{0.01}\right)_2O_4$	0.77	0.55
–	–	98.83	$\left(Fe^{2+}_{0.52}Mg_{0.51}Mn_{0.01}\right)_{1.03}\left(Cr_{1.22}Al_{0.68}Fe^{3+}_{0.09}Ti_{0.01}\right)_2O_4$	0.64	0.51
–	–	98.12	$\left(Fe^{2+}_{0.37}Mg_{0.67}\right)_{1.04}\left(Cr_{1.34}Al_{0.54}Fe^{3+}_{0.12}Ti_{0.01}\right)_2O_4$	0.71	0.66
–	–	99.10	$\left(Fe^{2+}_{0.41}Mg_{0.62}\right)_{1.04}\left(Cr_{1.34}Al_{0.55}Fe^{3+}_{0.1}Ti_{0.01}\right)_2O_4$	0.71	0.61
–	–	99.92	$\left(Fe^{2+}_{0.39}Mg_{0.64}\right)_{1.03}\left(Cr_{1.3}Al_{0.6}Fe^{3+}_{0.1}Ti_{0.02}\right)_2O_4$	0.68	0.64
0.28	–	99.67	$\left(Fe^{2+}_{0.57}Mg_{0.44}Mn_{0.01}Zn_{0.01}\right)_{1.03}\left(Cr_{1.1}Al_{0.8}Fe^{3+}_{0.1}Ti_{0.01}\right)_2O_4$	0.58	0.45
0.30	–	99.54	$\left(Fe^{2+}_{0.61}Mg_{0.39}Mn_{0.01}Zn_{0.01}\right)_{1.02}\left(Cr_{1.26}Al_{0.67}Fe^{3+}_{0.06}Ti_{0.01}\right)_2O_4$	0.66	0.40
–	–	99.74	$\left(Fe^{2+}_{0.57}Mg_{0.44}Mn_{0.01}\right)_{1.02}\left(Cr_{1.27}Al_{0.65}Fe^{3+}_{0.06}Ti_{0.01}\right)_2O_4$	0.66	0.44
–	–	99.64	$\left(Fe^{2+}_{0.62}Mg_{0.39}Mn_{0.01}\right)_{1.01}\left(Cr_{1.41}Al_{0.53}Fe^{3+}_{0.05}Ti_{0.01}\right)_2O_4$	0.73	0.39
–	0.13	99.96	$\left(Fe^{2+}_{0.54}Mg_{0.45}\right)_{0.99}\left(Cr_{1.46}Al_{0.52}Fe^{3+}_{0.01}Ti_{0.01}\right)_2O_4$	0.74	0.45
–	0.23	99.82	$\left(Fe^{2+}_{0.57}Mg_{0.41}Mn_{0.01}\right)_{0.99}\left(Cr_{1.47}Al_{0.5}Fe^{3+}_{0.01}Ti_{0.02}V_{0.01}\right)_2O_4$	0.74	0.42
–	0.01	99.74	$\left(Fe^{2+}_{0.56}Mg_{0.46}Mn_{0.01}\right)_{1.02}\left(Cr_{1.42}Al_{0.51}Fe^{3+}_{0.07}Ti_{0.01}\right)_2O_4$	0.74	0.46
0.01	0.22	99.82	$\left(Fe^{2+}_{0.54}Mg_{0.45}Mn_{0.01}\right)_{1.01}\left(Cr_{1.3}Al_{0.64}Fe^{3+}_{0.04}Ti_{0.02}V_{0.01}\right)_2O_4$	0.67	0.46
–	0.02	99.74	$\left(Fe^{2+}_{0.5}Mg_{0.5}Mn_{0.01}\right)_{1.01}\left(Cr_{1.27}Al_{0.68}Fe^{3+}_{0.03}Ti_{0.01}\right)_2O_4$	0.65	0.51

Analyses were performed with REMMA-202M SEM equipped with X-ray LZ-5 EDS, analyst V.A. Kotlyarov (nos. 1, 2, 7–20, 24–32) and with JEOL-733 SEM, analyst E.I. Churin (nos. 3–6, 20–23) at the Institute of Mineralogy, Ural Branch, Russian Academy of Sciences. Dash inducated not detected.

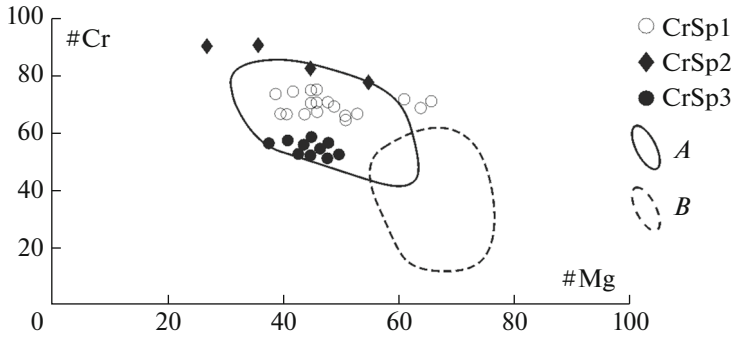

Fig. 6. Chemical compositions of Cr-spinels from Vladimir deposit plotted in classification chart (Irvine, 1965). (CrSp1) ore Cr-spinel; (CrSp2) latticed Cr-spinel; (CrSp3) relict accessory Cr-spinel. (*A*, *B*) fields of Cr-spinel from (*A*) peridotite of deepwater trench and (*B*) mid-ocean ridge.

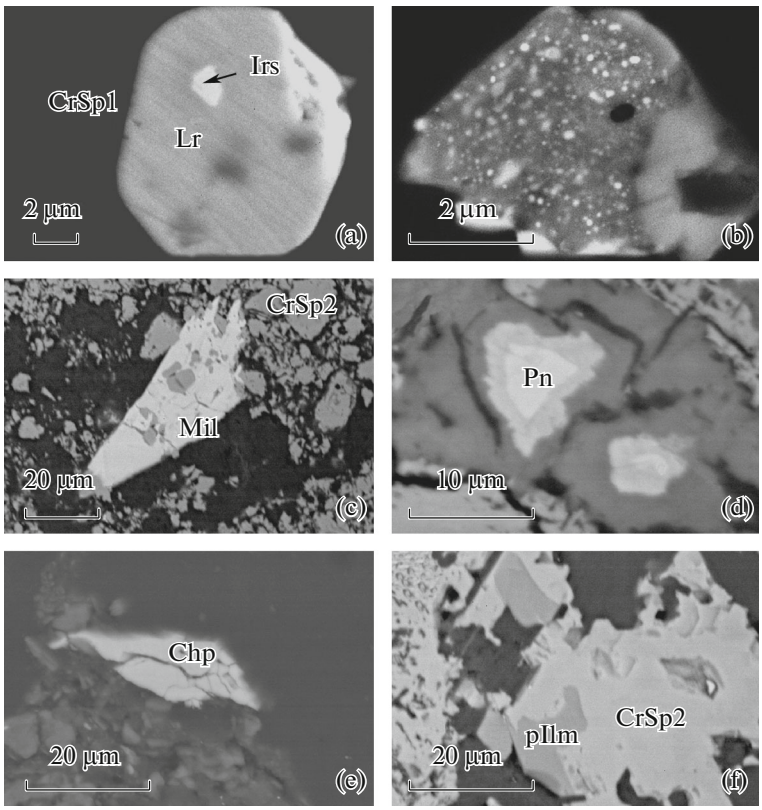

Fig. 7. Accessory mineralization in Cr-spinel at Vladimir deposit: (a) laurite crystal with iridisite inclusion in Cr-spinel (sample V-871-1); (b) complex intergrowth of Os, Ru, and Ir sulfides (sample V1-3b); (c) millerite with Cr-spinel microinclusions (sample 5vl-7); (d) zonal pentlandite in Cr-spinel (sample V-871-6); (e) chalcopyrite at boundary of Cr-spinel grain (sample 5vl-81); (f) picroilmenite inclusions in latticed high-chrome spinel (sample 5vl-49). BSE images: (a, b) JEOL JSM-7001F SEM, analysts O.V. Samoilova and M.V. Sudarikov; (c–f) REMMA-202M SEM, analyst V.A. Kotlyarov.

bearing packet as inclusions in accessory and ore-forming Cr-spinels. The chemical composition of the mineral is (wt %): 35–45 Ni, 20–30 Fe, and 32–34 S. Pentladite is commonly represented by a low-Co variety; Co admixture (up to 5%) was noted only in one case. Ni-rich pentlandite (Ni/Fe > 1.3) is more abundant; pentlandite proper is less abundant; the Fe-rich variety was not noted. Pentlandite grains are frequently zoned. The outer rim is depleted in Ni by 10–12 wt % and enriched in Fe and S by 6–7 and 4–5 wt %, respectively. The chemical composition of rims is not stoichiometric. The rims have sharp and readily discernible boundaries.

Chalcopyrite occurs as subhedral grains up to 30 μm long, which are not frequent as inclusions in Cr-spinel

Table 2. Results of X-ray spectroscopy of Ni, Fe, Pb, and Co sulfide and arsenide microinclusions in Cr-spinels at Vladimir deposit

No.	Polished section	Mineral	Number of analyses	Ni	Co	Fe	Cu	As	Pb	Sb	S	Total	Crystal chemical formula
1	5vl-88	Millerite	2	63.79	0.61	—	–	–	–	–	35.60	100.00	$(Ni_{0.98}Fe_{0.01})_{0.99}S$
2	5vl-79		3	58.40	–	7.19	–	0.92	–	–	33.35	99.87	$(Ni_{0.95}Fe_{0.12})_{1.07}(S_{0.99}As_{0.01})$
3	5vl-7		17	63.06	0.25	1.50	–	–	–	–	34.83	99.63	$(Ni_{0.99}Fe_{0.02})_{1.0}1S$
4	5vl-64		3	63.89	0.12	1.53	–	–	–	–	34.48	100.00	$(Ni_{1.01}Fe_{0.02})_{1.03}S$
5	5vl-73	Pentlandite	1	37.86	1.99	27.43	–	–	–	–	32.33	99.61	$(Ni_{5.12}Fe_{3.9}Co_{0.27})_{9.29}S_8$
6	V-871-6		5	33.52	3.08	29.82	–	–	–	–	33.39	99.81	$(Ni_{4.39}Fe_{4.1}Co_{0.4})_{8.89}S_8$
7	5vl-88		1	34.54	3.22	29.52	–	–	–	–	32.65	99.93	$(Ni_{4.62}Fe_{4.15}Co_{0.43})_{9.2}S_8$
8	5vl-79		4	42.35	0.40	23.16	–	0.53	–	–	33.57	100.00	$(Ni_{5.47}Fe_{3.16}Co_{0.02})_{8.65}(As_{0.06}S_{7.94})_8$
9	5vl-20		1	39.26	0.44	26.08	–	–	–	–	34.22	100.00	$(Ni_{5.01}Fe_{3.5}Co_{0.06})_{8.57}S_8$
10	5vl-82		3	35.53	1.63	28.61	–	–	–	–	33.63	99.41	$(Ni_{4.62}Fe_{3.91}Co_{0.21})_{8.74}S_8$
11	5vl-53		2	34.86	1.62	30.67	–	–	–	–	31.82	98.95	$(Ni_{4.79}Fe_{4.43}Co_{0.22})_{9.44}S_8$
12	5vl-84		7	34.54	2.25	29.75	–	–	–	–	33.15	99.69	$(Ni_{4.55}Fe_{4.12}Co_{0.3})_{8.7}S_8$
13	5vl-7		3	35.81	5.00	25.73	–	–	–	–	33.45	100.00	$(Ni_{4.68}Fe_{3.53}Co_{0.65})_{8.86}S_8$
14	5vl-62		1	44.18	—	22.33	–	–	–	–	33.33	99.84	$(Ni_{5.79}Fe_{3.08})_{8.87}S_8$
15	5vl-64		1	42.29	0.42	23.90	–	–	–	–	33.39	100.00	$(Ni_{5.53}Fe_{3.29}Co_{0.05})_{8.87}S_8$
16	5vl-55		1	45.43	1.45	20.77	–	–	–	–	31.83	99.49	$(Ni_{6.24}Fe_3Co_{0.2})_{9.44}S_8$
17	5vl-11		1	39.91	0.21	27.08	–	–	–	–	32.21	99.41	$(Ni_{5.41}Fe_{3.86}Co_{0.03})_{9.3}S_8$
18	5vl-81	Chalcopyrite	1	–	–	30.01	34.64	–	–	–	34.98	99.62	$Cu_{0.98}Fe_{0.98}S_2$
19	5vl-49	Maucherite	1	49.15	–	1.76	–	48.36	–	–	–	99.28	$(Ni_{10.38}Fe_{0.39})_{10.77}As_8$
20	5vl-85		1	47.54	0.48	2.51	–	49.73	–	–	–	100.00	$(Ni_{9.76}Fe_{0.49}Co_{0.1})_{10.35}As_8$
21			1	46.90	0.10	2.51	–	47.87	–	–	0.72	100.00	$(Ni_{9.66}Fe_{0.96}Co_{0.02})_{10.64}(As_{7.73}S_{0.27})_8$
22	5vl-49	Ni-As-S phase	1	61.57	–	2.51	–	7.01	–	–	27.99	99.07	
23	5vl-64	Pb-Ni-Cu-As-S phase	1	7.35	–	–	–	2.03	74.28	–	14.75	99.18	
24		Ni-Pb-As-S phase	1	40.97	–	–	–	28.22	12.79	–	16.82	100.00	
25		Ni-As-S phase	1	47.60	0.19	2.09	–	39.93	1.56	–	8.63	100.00	

Analyses were performed with REMMA-202M SEM equipped with X-ray LZ-5 EDS, analyst V.A. Kotlyarov. Dash indicates not detected.

(sample 5vl-81). The crystal chemical formula is close to stoichiometric.

Maucherite forms elongated grains up to 5 μm in size, which are often intergrown with millerite and the Ni–Fe–Co–As–S phase in various proportions. The chemical composition of maucherite is as follows (wt %): 47–49 Ni, 48.0–48.5 As, 2.0–4.5 Fe, occasionally with Co admixture. Mineral phases with complex compositions have been identified in latticed Cr-spinel as small grains up to 7 μm in size. Ni, Pb, Sb, As, and S are detected in various proportions.

The **Cr-bearing picroilmenite** occurs in latticed Cr-spinel as subhedral grains 15 μm in size. The Cr_2O_3 content varies from 1.6 to 2.5 wt %; V_2O_3 admixture is 0.1–0.9 wt % in concentration (Table 3). In addition, xenomorphic picroilmenite grains up to 100 μm in size are identified in spongy chromite–chlorite veinelts.

Laurite was identified in densely impregnated banded chromite ore (sample 871-1). The size of laurite grains is 10–12 μm; the shape is rounded with elements of faceting. The crystal chemical formula corresponds to a member of the laurite–erlichmanite series and differs in sulfur deficiency (Table 4), which can be caused by analytical uncertainties or submicroscopic native ruthenium inclusions. An inclusion of Ir sulfide with Rh, Ru, Cu, and Ni impurities has been identified by electron microscopy. This mineral is **comparable** in chemical composition with **kashinite** Ir_2S_3 and insufficiently characterized **iridisite** IrS_2. A complex intergrowth of small grains (~ 1 μm) represented by Os, Ru, and Ir sulfides has been revealed in ore vein (sample Vl-3b).

DISCUSSION

Composition and Alteration of Cr-spinels

First, let us emphasize the compositional differences of Cr-spinel types (Fig. 3). The ore-forming varieties are medium-chrome and contain 49–56 wt % Cr_2O_3. They are only slightly affected by transformations manifested in the appearance of thin Cr-magnetite rims and veinlets. The latticed Cr-spinel with chlorite ingrowths is high-chrome (57–67 wt % Cr_2O_3). Wide Cr-magnetite rims are inherent to accessory Cr-spinel. Gradual growth of rims gives rise to the formation of complete Cr-magnetite and magnetite pseudomorphs after Cr-spinel. Cr-magnetite is markedly depleted in Cr_2O_3, Al_2O_3, and MgO along with enrichment in Fe_2O_3 and MnO. Removed chromium has been recorded in the host chlorite and serpentinite. Rounded Cr-spinel relics enriched in Al_2O_3 and containing 38–43 wt % Cr_2O_3 are retained in grain cores. These relics are close to Cr-picotite in composition. These geochemical signatures are typical of ultramafic complexes and widely highlighted in the literature (Kashin, 1937; Bazhin et al., 2010).

Table 3. Results of X-ray spectroscopy of picroilmenite inclusions in Cr-spinels at Vladimir deposit

Polished section	Mineral	Grain	TiO_2	MgO	FeO	Cr_2O_3	MnO	V_2O_3	Al_2O_3	Total	Crystal chemical formula
5vl-49	Picroilmenite	1	61.25	12.39	25.05	0.42	0.38	–	0.01	99.51	$(Mg_{0.42}Fe_{0.47}Mn_{0.01})_{0.9}(Ti_{1.04}Cr_{0.01})_{1.05}O_3$
		2	59.70	12.94	24.53	1.57	0.43	–	0.06	99.23	$(Mg_{0.44}Fe_{0.47}Mn_{0.01})_{0.92}(Ti_{1.02}Cr_{0.03})_{1.05}O_3$
		3	60.95	13.46	22.11	2.49	0.47	–	0.06	99.55	$(Mg_{0.45}Fe_{0.41}Mn_{0.01})_{0.87}(Ti_{1.03}Cr_{0.04})_{1.05}O_3$
		4	61.40	12.61	22.93	2.27	0.33	0.11	0.04	99.68	$(Mg_{0.42}Fe_{0.43}Mn_{0.01})_{0.86}(Ti_{1.04}Cr_{0.04})_{1.08}O_3$
		5	60.42	13.31	22.56	2.08	0.51	0.42	0.10	99.39	$(Mg_{0.45}Fe_{0.42}Mn_{0.01})_{0.88}(Ti_{1.02}Cr_{0.04})_{1.06}O_3$
		6	61.65	13.71	22.09	1.67	0.42	0.38	0.07	99.96	$(Mg_{0.46}Fe_{0.41}Mn_{0.01})_{0.88}(Ti_{1.03}Cr_{0.03})_{1.06}O_3$
		7	61.47	13.57	22.15	1.77	0.48	0.49	0.01	99.94	$(Mg_{0.45}Fe_{0.41}Mn_{0.01})_{0.87}(Ti_{1.03}Cr_{0.03})_{1.06}O_3$

Analyses were performed with REMMA-202M SEM equipped with X-ray LZ-5 EDS, analyst V.A. Kotlyarov. Dash indicates not detected. Grains 1, 2, with three analyses; grain 6, by two analyses; grains 3–5, 7 by one analysis.

Table 4. Results of X-ray spectroscopy of PGE sulfide microinclusions in Cr-spinels at Vladimir deposit

No.	Polished section	Mineral	Number of analyses	Ru	Os	Ir	Rh	Pt	Ni	Cu	Fe	As	S	Total	Crystal chemical formula
1	871-1	Laurite–erlichmanite	5	39.86	15.27	13.38	—	—	—	—	—	—	31.48	100.00	$(Ru_{0.80}Os_{0.16}Ir_{0.14})_{1.1}S_2$
2	V1-3B	The same	3	44.81	17.43	4.15	—	—	0.15	—	1.23	0.79	31.44	100.00	$(Ru_{0.89}Os_{0.18}Ir_{0.04}Fe_{0.04}Ni_{0.01})_{1.16}(S_{1.98}As_{0.02})_2$
3	V1-3B-1	The same	4	52.14	8.47	5.46	—	—	0.79	—	1.08	1.90	30.18	100.02	$(Ru_{1.07}Os_{0.09}Ir_{0.06}Fe_{0.04}Ni_{0.03})_{1.29}(S_{1.95}As_{0.05})_2$
4	V1-3B-2	Laurite	3	26.18	—	32.89	—	—	0.36	—	5.73	13.67	21.43	100.25	$(Ru_{0.67}Ir_{0.40}Fe_{0.24}Ni_{0.01})_{1.27}(S_{1.57}As_{0.43})_2$
5	V1-3B-3	Laurite–erlichmanite	2	47.32	16.47	6.98	—	—	0.96	—	1.33	1.50	24.46	99.02	$(Ru_{1.12}Os_{0.21}Ir_{0.09}Fe_{0.06}Ni_{0.04})_{1.16}(S_{1.95}As_{0.05})_2$
6	871-1-1	Kashinite	1	8.76	—	48.17	8.60	—	6.73	1.60	—	—	26.14	100.00	$(Ir_{0.92}Ru_{0.32}Rh_{0.31}Ni_{0.42}Cu_{0.10})_{2.07}S_3$
7	871-1-2	The same	1	7.83	—	45.68	8.98	7.00	6.41	—	—	—	23.80	100.00	$(Ir_{0.96}Rh_{0.35}Ru_{0.31}Ni_{0.44}Pt_{0.15})_{2.22}S_3$

Analyses were performed with JEOL JSM-7001F SEM, analysts M.V. Sudarikov and O.V. Samoilova at the Electron Microscopy Laboratory of the Southern Ural Geological Administration. Dash indicates not detected.

Relationship between Metamorphism and Metasomatism in the Cr-Spinel Transformation

The Vladimir deposit is related to the serpentinite type of chromite occurrences in geological, morphological, and petrographic attributes (Saveliev, 2012). The orebodies are localized in antigorite, chrysotile, and antigorite–bastite–chrysotile serpentinites. In the chemistry of Cr-spinel, the Vladimir deposit is pertaining to the alumina type like other deposits of the Varshavsky massif, as well as chromite deposits localized in other massifs of the East Ural Megazone (Verblyuzhy Mountains,Tatishchevo).

Alekseev (2005) carried out a targeted study of the influence of metamorphism on ultramafic rocks of the Verblyuzh'egorsky massif, located 40–50 km from the Vladimir deposit. According to his data obtained with use of an olivine–Cr-spinel geothermometer, high-temperature (900–450°C) and low-temperature (400–300°C) types of metamorphism have been recorded. The former is related to the effect of Middle Paleozoic gabbroic rocks, and the latter, to the Late Paleozoic collision.

At the Vladimir deposit, the transformation of ore-forming Cr-spinels is manifested in the appearance of high-chrome latticed varieties with chlorite ingrowths and Cr-magnetite and magnetite rims. They are similar to high-grade metamorphic varieties of the Verbluzh'egorsky massif; however, a cause of their appearance is different, related to the effect of the fluid–thermal field of the Varshavsky granitic pluton with accompanying dikes and hydrothermal phenomena (Fig. 1). As shown above, a granite porphyry dike is exposed in the open pit. Extensive fields of talc–carbonate metasomatic rocks develop in its framework.

Since latticed Cr-spinel occurs locally in marginal parts of orebodies, they are a result of hydrothermal activity, which also leads to the appearance of chlorite selvage at the peripheries of orebodies. The change in the Cr-spinel composition, manifested in thin rims of Cr-magnetite and magnetite proper, are referred to low-temperature metamorphism.

Composition and Location of Accessory Mineralization

The set of accessory ore minerals identified at the Vladimir deposit comprises sulfides, Ni and Fe arsenides, picroilmenite, and quite rare PGE sulfides and native gold and nickel.

Native nickel is found in nature extremely rarely; awaruite and nickel–iron are more abundant. Our precursors revealed native nickel in miarolic pegmatites of the Lower Tagil Pluton (Pushkarev, et al., 2007) and in chromite ore at the Central I deposit in the Polar Urals in association with native gold and minerals from the laurite–erlichmanite series (Pasava et al., 2011). The origin of native nickel at the Vladimir deposit is likely related to transformation of the abun-

dant Ni sulfides and arsenides during serpentinization of this massif.

Native gold inclusions have been revealed in chromite of the Kraka massif in the southern Urals (Kovalev et al., 2007). Gold from the Vladimir deposit in the Varshavsky massif is close in composition to gold from the Khamitovo and Sarangaevo deposits in the Kraka massif. In the latter case, native gold contains (wt %): 89–90 Au, 7–8 Ag, and 1–3 Cu. Mineralization has been established at the roof and the bottom of the chromite-bearing packet.

It has been suggested that gold concentrated from ultramafic rocks themselves in the course of their transformation, including tectonic fragmentation, fissility, and antigoritization (Sazonov, 1999). Gold at the Vladimir deposit, which was found in a fracture at the contact of chromite ore and serpentinite, is also secondary in origin and most likely related to hydrothermal activity.

Picroilmenite is widespread in both deep-rooted rocks and currently shallow-seated metamorphosed ultramafic massifs. Picroilmenite and geikielite are associated with high-Ti Cr-spinel (no less than 1% TiO_2) (Pushkarev, 2000). At the Vladimir deposit, picroilmenite has been identified in latticed Cr-spinel with lower TiO_2 content (0.3–1.0 wt %). The occurrence of picroilmenite exclusively in latticed Cr-spinel indicates the possible transition of Ti compounds to an independent mineral phase under the action of high temperature.

Laurite is known in the Urals at primary and placer deposits of the Platinum Belt (*Mineralogiya ...*, 1990). In the southern Urals, laurite has been identified in the Nurali massif at the Priozerny occurrence (*Platinometallnoe ...*, 2001; Grieco et al., 2001). Minerals of the laurite–erichmanite series enriched in Ir and Rh have been found in cataclastic densely impregnated chromite ore. The homogeneous grains are combined with euhedral crystals with complex zoning caused by replacements between Os and Ir. The study of laurite segregations in chromite ore of the Milia region (ophiolites, Greece) has shown that chromite ore crystallized from an ultramafic melt (Kapsiotis et al., 2009). Kashinite has been described from Solov'eva Gora, Aleksandrov Log, and other ore objects near Nizhny Tagil. Ru, Pt, Cu, and Fe are common admixtures. A mineral assemblage comprising platinum, iridosmine, erlichmanite, cuproiridsite, laurite, Fe, Cu, and Rh sulfides, and chromite is typical (Begizov et al., 1985). A mineral revealed by us contains Ni as an impurity; excess cations are apparently explained by microingrowths of native PGM. The complex intergrowth of small individuals composed of Os, Ru, and Ir sulfides is attractive. Similar intergrowths were revealed earlier in the weathering mantle at Cu–Ni deposits in Spain (Suarez et al., 2010).

CONCLUSIONS

Cr-spinels from the Vladimir deposit are represented by three main types: (i) medium-chrome ore-forming, (ii) high-chrome latticed, and (iii) low-chrome accessory. Ore-forming Cr-spinel making up banded and veined ore bodies contains 48–57 wt % Cr_2O_3. High-chrome latticed Cr-spinel containing 58–62 wt % Cr_2O_3 is localized at the margins of orebodies and nephrite-like serpentinite. Its formation is apparently caused by the influence of the fluid–thermal field of the Varshavsky granitic pluton and concomitant dikes and hydrothermal phenomena. In accessory grains (38–45 wt % Cr_2O_3), Cr-spinel relics have been retained only in their cores, which are surrounded by a Cr-magnetite rim. The transformation of Cr-spinel was completed during development of the weathering mantle.

The accessory minerals revealed at the Vladimir deposit are represented by PGM and native gold and nickel; Fe, Ni, and Co sulfides; picroilmenite; and complex polymetallic phases. Accessories are associated with transformed types of Cr-spinels, primarily with the high-chrome latticed type.

ACKNOWLEDGMENTS

We thank E.V. Belogub, L.Ya. Kabanova, E.I. Churin, O.V. Samoilova, and M.V. Sudarikov for their assistance in preparation of this paper. The study was supported by the Russian Science Foundation (project no. 16-18-10322) and the State Program of the Ministry of Education and Science of the Russian Federation (no. 33.2644.2014k).

REFERENCES

Alekseev, A.V., *Conditions of formation and composition of chromite ores of Alapaevsk, Verh-Neyvinsky and Verblyuzhegorsky alpine ultrabasic massifs of the Urals, Extended Abstract in Geology and Mineralogy*, Yekaterinburg: IGG UB of RAS, 2005.

Bazhin, E.A., Saveliev, D.E., and Snachev, V.I., *Gabbro-giperbazitovye kompleksy zony sochleneniya Magnitogorskoi i Tagil'skoi megazon: stroenie i usloviya formirovaniya*, (The Gabbro–Ultrabasite Complex from the Tagil and Magnitogorsk Megazone Junction: Geology and Conditions of Formation), Ufa: DizaynPoligrafServis, 2010.

Grieco, G., Ferrario, A. Diella, V., Spadea, P., Savelieva, J., Pertsev N., and Mather E.A., The Cr-PGE mineralization of the Nurali massif, Southern Urals, Russia, in *Postcollision evolution of mobile belts, Abstr. Int. Sci. Conf.* Yekaterinburg: IGG UB of RAS, 2001. P. 60—62.

Irvine, T.N., Chromian spinel as a petrogenetic indicator. Part I: Theory, *Can. J. Earth Sci*, 1965, vol. 2, p. 648.

Kapsiotis, A., Grammatikopoulos, T., Tsicouras, B., Hatzipanagiotou, K., Zaccarini, F., and Garuti, G., Chromian spinel composition and platinum-group element mineralogy of chromites from the Milia Area, Pindos ophiolite complex, Greece, *Can. Mineral.*, 2009, vol. 47, p. 1057.

Kashin, S.A., Metamorphism of chromium spinelides in chromite deposits of Verbluzhie Mountains (the Southern Urals), in *Khromity SSSR (Chromites of the USSR)*, Moscow–Leningrad: Akad. Nauk SSSR, 1937, Vol. 1, pp. 251–338 (in Russian).

Kovalev, S.G., Chernikov, A.P., and Burdakov, A.V., First finding of native gold in chromites from rock massifs of Kraka (Southern Urals), *Dokl. Earth Sci.*, 2007, vol. 414, no. 4, p. 526–530.

Mineralogiya Urala. Elementy. Karbidy. Sul'fidy (Mineralogy of the Urals. Elements. Carbides), Sverdlovsk: Ur. Otd. Akad. Nauk SSSR, 1990.

Ovchinnikov, L.N., *Poleznye iskopaemye i metallogeniya Urala* (Mineral Resources and Metallogeny of the Urals), Moscow: Geoinformmark, 1998.

Pasava, J., Knesl, I., Vymazalova, A., Vavrin, I., Gurskaya, L.I., and Kolbantsev, L.R., Geochemistry and mineralogy of platinum-group elements (PGE) in chromites from Centralnoye I, Polar Urals, Russia, *Geosci. Front.*, 2011, no. 2, p. 81–85.

Pavlov, N.V., *Khimicheskii sostav khromshpinelidov v svyazu s oetrografichesim sostavom porod ul'traosnovnyikh intruzivov* (The Chemical Composition of Chromium Spinelides in Connection with the Petrographic Composition of the Ultramafic Intrusion Rocks), *Tr. Geol. Inst. Ross. Akad. Nauk*, 1949, vol. 103.

Platinometallnoe orudenenie v geologichskikh kompleksakh Urala (PGM Mineralization in the Geological Complexes of the Urals), Koroteev, V.A. and Zoloev, K.K., Yekaterinburg, 2001.

Pushkarev, E.V., *Petrologiya Uktusskogo dunit–gartsburgit–gabbrovogo massiva* (Petrology of the Uktus Dunite–Harzburgite–Gabbro Massif (the Middle Urals), Yekaterinburg: IGG UB of RAS, 2000, p. 291.

Pushkarev, E.V., Anikina, E.V., Garuti, G., and Zakkarini, F., Cromium-platinum deposits of Nizhny-Tagil type in the Urals: structural-substantial characteristic and a problem of genesis, *Litosfera*, 2007, no. 3, p. 28.

Saveliev, D.E., *Chromite Potential of Ultramafic Complexes of the Southern Urals*, Doctoral Dissertation in Geology and Mineralogy, Ufa, 2012.

Sigov, A.P., *Metallogeniya mezozoya i kainozoya Urala* (Metallogeny of the Mesozoic and Cenozoic of the Urals), Moscow: Nedra, 1969.

Suarez, S., Prichard, H., Velasco, F., Fisher, P., and McDonald, I., *Alteration of platinum-group minerals and dispersion of platinum-group elements during progressive weathering of the Aguablanca Ni-Cu deposit, SW Spain*, *Miner. Deposita*, 2010, p. 331–350.

Zaykov, V.V., Melekeszeva, I.Yu., Artem'ev, D.A., Yuminov, A.M., Simonov, V.A., and Dunaev, A.Yu., *Geologiya i kolchedannoe orudenenie yuzhnogo flanga Glavnogo Ural'skogo razloma,* (Geology and Sulphide Mineralization of the Southern Flank of the Main Ural Fault), Miass: IM Ural. Otd. Ross. Akad. Nauk, 2009.

Translated by V. Popov